Boada, Beatriz L.; Boada, María Jesús L.; Vargas-Meléndez, Leandro; Díaz, Vicente. *A robust observer based on H_∞ filtering with parameter uncertainties combined with Neural Networks for estimation of vehicle roll angle.* Mechanical Systems and Signal Processing, 99 (2018), pp. 611-623

DOI: https://doi.org/10.1016/j.ymssp.2017.06.044

A robust observer based on H_∞ filtering with parameter uncertainties combined with Neural Networks for estimation of vehicle roll angle

Abstract

Nowadays, one of the main objectives in road transport is to decrease the number of accident victims. Rollover accidents caused nearly 33% of all deaths from passenger vehicle crashes. Roll Stability Control (RSC) systems prevent vehicles from untripped rollover accidents. The lateral load transfer is the main parameter which is taken into account in the RSC systems. This parameter is related to the roll angle, which can be directly measured from a dual-antenna GPS. Nevertheless, this is a costly technique. For this reason, roll angle has to be estimated. In this paper, a novel observer based on H_∞ filtering in combination with a neural network (NN) for the vehicle roll angle estimation is proposed. The design of this observer is based on four main criteria: to use a simplified vehicle model, to use signals of sensors which are installed onboard in current vehicles, to consider the inaccuracy in the system model and to attenuate the effect of the external disturbances. Experimental results show the effectiveness of the proposed observer..

Keywords: vehicle dynamics, roll angle estimation, NN, robust observer, H_∞ observer.

1. Introduction

Nowadays, one of the main objectives in road transport is to decrease the number of accident victims. For this reason, present vehicles are equipped with control systems, such as ESC (Electronic Stability Control) and RSC (Roll Stability Control) [1][2], in order to improve the vehicle safety. These systems need to know in advance the expected vehicle behaviour during different conditions and manoeuvres to properly actuate on these control systems [3][4][5]. Specifically, knowledge of the vehicle roll angle is useful in RSC systems. Rollover accidents caused nearly 33% of all deaths from passenger vehicle crashes [6]. The main objective of the RSC systems is to stabilize to maximize the roll stability of the vehicle. Roll stability is achieved if the tires are in contact with the ground. This condition is achieved when the normalized load transfers for both axles, R_i, (i = front, rear) are below the value ± 1 [2]:

$$R_i = \frac{LLT_i}{F_{zi}} \tag{1}$$

where F_{zi} is the total axle load and LLT_i is the Lateral Load Transfer in each axle (front and rear) which can be given by the equation:

$$LLT_i = \frac{k_i \cdot \phi}{T} \tag{2}$$

where k_i is the roll stiffness at the front and rear axles, ϕ is the roll angle of the sprung mass and T is the vehicle track width. The normalized load transfer value, R_i, corresponds to the largest possible load transfer. If the R_i takes on the value $\pm$ 1, then the inner wheels in the bend lift off. The limit cornering condition occurs when the load on the inside wheels has dropped to zero and all the load has been transferred onto the outside wheels. The success of

RSC system will depend of knowledge of vehicle roll angle. The vehicle roll angle can be directly measured from a dual-antenna GPS. Nevertheless, this is a costly technique. For this reason, roll angle has to be estimated [7][8]. In [9], an algorithm for estimating the roll angle is proposed which uses the measurements obtained from accelerometers and suspension deflection sensors. However, this method doesn't provide very accurate estimations [8]. Furthermore, suspension deflection sensors are expensive, so they are typically not available for vehicles [7]. In [7], a dynamic observer which used the information obtained from a lateral accelerometer and a gyroscope is proposed. However, the estimated vehicle roll angle transient response has an important error. In this algorithm, neither measurement nor model noises are taken into account. Other authors use low-cost GPS and onboard vehicle sensors in order to estimate the vehicle roll angle [10][11]. However, the problem of using GPS is to get a high accuracy readings and visibility of the satellites in both urban and forested driving environments [12].

In [8] [12] [13] [14], the Kalman Filter is used for estimation of vehicle roll angle. The Kalman filter is an iterative method to optimally estimates the states of a system from noisy sensor measurements. The problem is that it is necessary that the system model is precise and that the statistical information, referred to noise of both the model and the measurements, is given. When this doesn't occur, the performance of Kalman Filter may degrade [15].

Assuming that the noise is bounded, a robust observer design is an effective way in dealing with system uncertainties and the parameters variations [16]. Typically, there are three strategies in the robust filtering: energy-

to-energy filtering (H_∞), peak-to-peak filtering and energy-to-peak filtering [17][18]. In the energy-to-energy filtering, the noise is arbitrary but with bounded energy. In peak-to-peak filtering, the worst case peak value of the estimation error for the bounded peak value of noise is minimized. Finally, in the energy-to-peak filtering, the estimation of error is minimized for any bounded energy disturbance. Some authors propose robust controllers for improving the vehicle behaviour [19] [20] [21] and others propose robust observers for vehicle sideslip angle estimation [17] [22].

However, there is a lack of research about the robust vehicle roll angle estimation. We aim to develop a robust observer based on H_∞ filtering in combination with a neural network (NN) for the vehicle roll angle estimation. The design of this observer is based on four main criteria:

- to use in all types of environments (tunnels, urban and forested driving environments),
- to use a simplified vehicle model,
- to use signals of sensors that they are installed onboard in current vehicles,
- to consider the inaccuracy in the system model and
- to attenuate the effect of the external disturbances.

The NN estimates a "pseudo-roll angle" through measurements obtained by affordable physical sensors and this value is introduced in robust H_∞-based observer in order to reduce not only the system uncertainty but also

to reduce the effect of external disturbances. Experimental results show the necessity of estimating the "pseudo-roll angle" previously.

This paper is organized as follows. The vehicle model for observer design is described in Section 2. A simplified roll vehicle model is used in order to reduce the computing time. Moreover, the parameter uncertainties are considered. In Section 3, a description of proposed observer is given. A novel observer based on Neural Networks (NN) combined with a robust H_∞ filtering is described. In Section 4, a description of the real vehicle and the sensors mounted on it is given. In addition, the proposed observer is analyzed using real experiments and the results are shown. Finally, the summary and conclusions are given in Section 5.

2. Vehicle model

We consider a 1-DOF (Degree Of Freedom) vehicle model which is widely adopted to describe the vehicle roll motion (Figure 1). In the model, a fixed coordinate system (x, y, z) is adopted in order to describe the vehicle roll motion. It is assumed that the vehicle sprung mass rotates around the roll centre of the vehicle. The vehicle's roll dynamic is governed by the following differential equation [8]:

$$I_{xx}\ddot{\phi} + C_R\dot{\phi} + K_R\phi = m_s a_y h_{cr} + m_s h_{cr} g \sin(\phi) \tag{3}$$

where ϕ is the vehicle roll angle, I_{xx} is the sprung mass moment of inertia with respect to the roll axis, m_s is the sprung mass, h_{cr} is the sprung mass height about the roll axis, C_R represents the total torsional damping, K_R is the stiffness coefficient, a_y represents the lateral acceleration at the vehicle Center Of Gravity (COG) and g is the acceleration due to gravity.

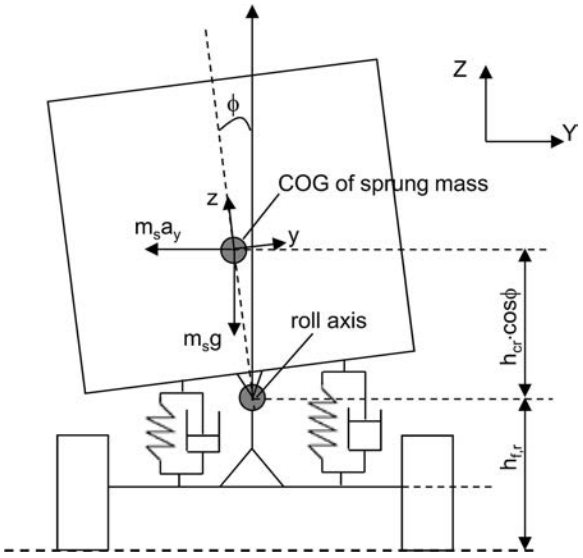

Figure 1: Vehicle roll model.

Nowadays, vehicles incorporate many sensors such as accelerometers and rate sensors. Since accelerometers provide measurements of acceleration due to gravity as well as the vehicle's acceleration, the relation between the lateral acceleration measured by the sensor (a_{ym}) and the vehicle lateral acceleration (a_y) is given by:

$$a_{ym} = g \sin(\phi) + a_y \cos(\phi) \tag{4}$$

Considering that the vehicle roll angle is small, the following approximations are used:

$$\sin(\phi) \approx \phi \tag{5}$$

$$\cos(\phi) \approx 1 \tag{6}$$

the measured lateral acceleration (a_{ym}) can be written as:

$$a_{ym} = a_y + g\phi \tag{7}$$

Considering above approximations, Eq. 3 can be rewritten as:

$$I_{xx}\ddot{\phi} + C_R\dot{\phi} + K_R\phi = m_s a_{y_m} h_{cr} \tag{8}$$

In addition, the pitching and the bounding motions of the sprung mass are assumed to be neglected and the road bank angle is assumed to be small, then the vehicle roll rate ($\dot{\phi}$) is considered equal to the roll rate given by the sensor ($\dot{\phi}_m$):

$$\dot{\phi} = \dot{\phi}_m \tag{9}$$

A state-space model of the vehicle roll dynamic can be represented as:

$$\begin{aligned} \dot{\mathbf{x}}_0 &= \mathbf{A}_0\mathbf{x}_0 + \mathbf{B}_0 a_{ym} + \mathbf{H}\mathbf{w} \\ \mathbf{y} &= \mathbf{C_0}\mathbf{x}_0 + \mathbf{q} \end{aligned} \tag{10}$$

where $\mathbf{x}_0$ represents the state vector, $[\phi, \dot{\phi}]^T$, $\mathbf{y}$ is the measurement vector, w is the disturbance, $\mathbf{q}$ is the measurement noise and,

$$\mathbf{A}_0 = \begin{bmatrix} 0 & 1 \\ -K_R/I_{xx} & -C_R/I_{xx} \end{bmatrix} \tag{11}$$

$$\mathbf{B}_0 = \begin{bmatrix} 0 \\ m_s h_{cr}/I_{xx} \end{bmatrix} \tag{12}$$

$$\mathbf{H} = \mathbf{I}_{2x2} \tag{13}$$

Since, the parameters $[I_{xx}, m_s, C_R, K_R, h_{cr}]$ cannot be measured easily and precisely, and even they can vary over time, hence, the system can be rewritten as:

$$\begin{aligned} \dot{\mathbf{x}}_0 &= (\mathbf{A}_0 + \Delta\mathbf{A}_0)\,\mathbf{x}_0 + (\mathbf{B}_0 + \Delta\mathbf{B}_0)\,a_{ym} + \mathbf{H}\mathbf{w} \\ \mathbf{y} &= \mathbf{C_0}\mathbf{x}_0 + \mathbf{q} \end{aligned} \tag{14}$$

$\Delta\mathbf{A}_0$ and $\Delta\mathbf{B}_0$ represent the system uncertainties for matrices $\mathbf{A}_0$ and $\mathbf{B}_0$:

$$\begin{aligned}\mathbf{A}_0 + \Delta\mathbf{A}_0 &= \begin{bmatrix} 0 & 1 \\ \frac{-(K_R+\Delta K_R)}{(I_{xx}+\Delta I_{xx})} & \frac{-(C_R+\Delta C_R)}{(I_{xx}+\Delta I_{xx})} \end{bmatrix} \\ \mathbf{B}_0 + \Delta\mathbf{B}_0 &= \begin{bmatrix} 0 \\ \frac{(m_s+\Delta m_s)(h_{cr}+\Delta h_{cr})}{(I_{xx}+\Delta I_{xx})} \end{bmatrix}\end{aligned} \tag{15}$$

In order to reduce the complexity of the problem, the following considerations have been taking into account:

$$\frac{a+\Delta a}{b+\Delta b} = \frac{a}{b+\Delta b} + \frac{\Delta a}{b+\Delta b} \approx \frac{a}{b} + \frac{\Delta a}{b} \tag{16}$$

$$(c+\Delta c)(d+\Delta d) = cd + c\Delta d + \Delta cd + \Delta c\Delta d \approx cd + c\Delta d + \Delta cd \tag{17}$$

Then, the uncertainties matrices can be rewritten as:

$$\Delta\mathbf{A}_0 = \mathbf{E}_A \cdot \mathbf{M} \cdot \mathbf{F}_A \tag{18}$$

$$\Delta\mathbf{B}_0 = \mathbf{E}_B \cdot N(t) \cdot \mathbf{F}_B \tag{19}$$

where,

$$\mathbf{E}_A = \begin{bmatrix} 0 & 0 \\ \frac{-\Delta K_R}{I_{xx}} & \frac{-\Delta C_R}{I_{xx}} \end{bmatrix} \tag{20}$$

$$\mathbf{F}_A = \mathbf{I}_{2x2} \tag{21}$$

$$\mathbf{E}_B = \begin{bmatrix} 0 \\ \frac{\Delta m_s h_{cr} + m_s \Delta h_{cr}}{I_{xx}} \end{bmatrix} \tag{22}$$

$$\mathbf{M} = \begin{bmatrix} N(t) & 0 \\ 0 & N(t) \end{bmatrix} \tag{23}$$

$$|N(t)| \leq 1 \tag{24}$$

$$\mathbf{F}_B = \mathbf{I}_{1x1} \tag{25}$$

where ΔK_R, ΔC_R, Δh_{cr} and Δm_s are the maximum uncertainties of K_R, C_R, h_{cr} and m_s, respectively.

3. Proposed observer based on $\mathbf{H_\infty}$ filtering combined with neural networks

The roll angle is an essential parameter whose knowledge is fundamental for vehicle rollover controlling behaviour. Hence, a novel observer based on H_∞ filtering in combination with Neural Network (NN) for the estimation of the vehicle roll angle is proposed. The proposed observer architecture is shown in Figure 2. The estimation process consists of two blocks: the first block serves to estimate the vehicle roll angle using NN. The NN module acts as a "pseudo-sensor" providing a "pseudo-roll angle" through other measurements obtained by physical on-board vehicle sensors. The design of a NN-based "pseudo-sensor" is useful in order to avoid the use of sensors which provide directly the vehicle roll angle. The problems of these types of sensors are that they are very costly and they used the information given by GPS system. The "pseudo-roll angle" information is necessary to be introduced in the H_∞-based observer in order to obtain a good estimation of vehicle states. The second block contains an H_∞ state estimation that uses the result of the first block to consider the uncertainties of parameters and to attenuate the effect of the disturbances of measurement obtained from the first block. In this case, the pseudo-roll angle is estimated from the observer based on NN.

As the NN used is a static NN, the error of the NN can be assumed as

a "pseudo-sensor" noise. The advantage of the H_∞-based observer used in this research is that the knowledge about the sensor noise is not required contrary to Kalman Filter. Hence, the analysis of convergence of the proposed algorithm (NN+H_∞ observer) is reduced to analyze the converge of H_∞ observer.

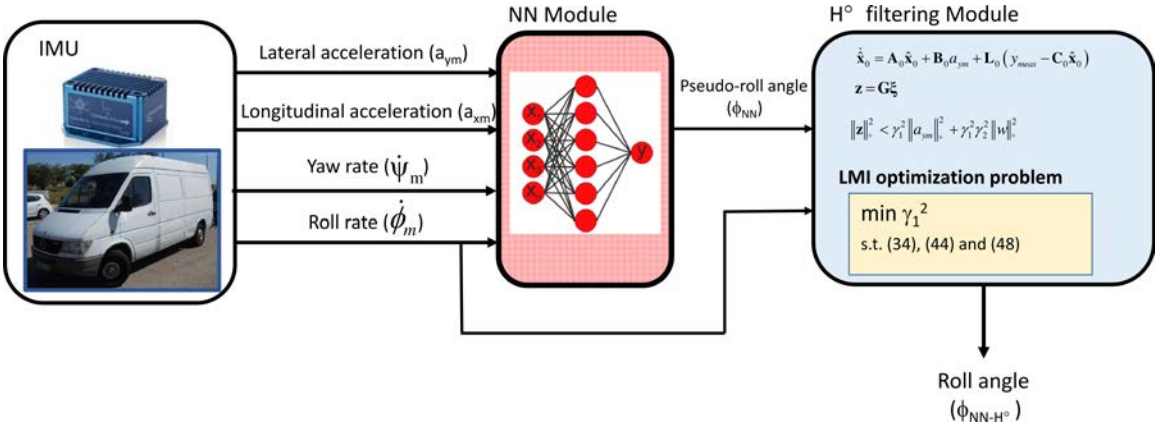

Figure 2: Observer architecture

3.1. Neural Network Module

This module corresponds with the design of an artificial neural network which provides a "pseudo-roll angle" using the signals of inertial sensors that they are installed on-board in current vehicles. The architecture of the NN is depicted in Figure 3. The NN is formed by a single hidden layer with 15 neurons, four inputs corresponding to the the longitudinal acceleration, a_{xm}, the lateral acceleration, a_{ym}, the yaw rate , $\dot{\psi}_m$, and the roll rate, $\dot{\phi}_m$ and one output corresponding to the vehicle "pseudo-roll angle", ϕ_{NN}. A detailed description about the training of NN and results obtained is given in [8].

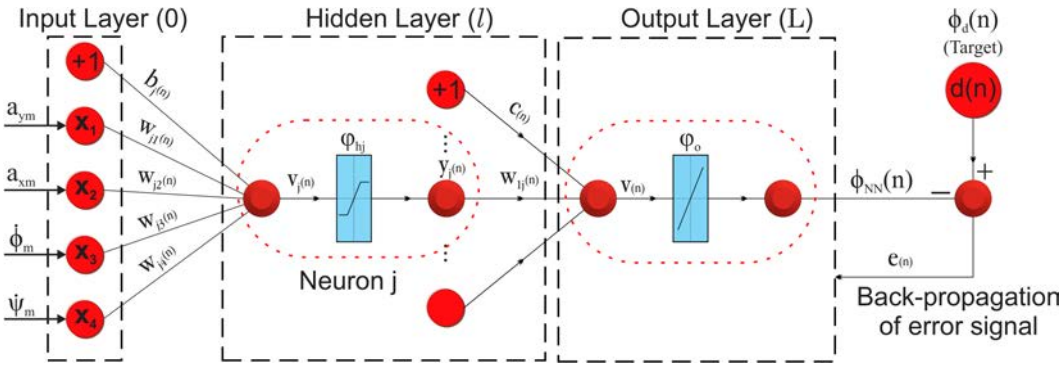

Figure 3: Observer architecture

3.2. H_∞ filtering observer Module

To estimate the vehicle roll angle, we define an observer which has the following form:

$$\dot{\hat{\mathbf{x}}}_0 = \mathbf{A}_0\hat{\mathbf{x}}_0 + \mathbf{B}_0 a_{ym} + \mathbf{L}_0\left(\mathbf{y}_{meas} - \mathbf{C}_0\hat{\mathbf{x}}_0\right) \tag{26}$$

where $\mathbf{y}_{meas}$ is the measurements or pseudo-measurements obtained directly by vehicle sensors and $\mathbf{L}_0$ is the observer gain to be determined. The estimation error of states is defined as:

$$\mathbf{e} = \mathbf{x}_0 - \hat{\mathbf{x}}_0 \tag{27}$$

hence, the estimation error dynamic is expressed as:

$$\dot{\mathbf{e}} = \dot{\mathbf{x}}_0 - \dot{\hat{\mathbf{x}}}_0 \tag{28}$$

By substituting Eq. (14) and Eq. (26) in Eq. (28),

$$\begin{aligned}\dot{\mathbf{e}} = \quad & \left(\mathbf{A}_0 + \Delta\mathbf{A}_0\right)\mathbf{x}_0 + \left(\mathbf{B}_0 + \Delta\mathbf{B}_0\right)a_{ym} + \mathbf{H}\mathbf{w} - \\ & - \left(\mathbf{A}_0\hat{\mathbf{x}}_0 + \mathbf{B}_0 a_{ym} + \mathbf{L}_0\left(\mathbf{y}_{meas} - \mathbf{C}_0\hat{\mathbf{x}}_0\right)\right)\end{aligned} \tag{29}$$

and operating,

$$\dot{\mathbf{e}} = (\mathbf{A}_0 - \mathbf{L}_0\mathbf{C}_0)\,\mathbf{e} + \Delta\mathbf{A}_0\mathbf{x}_0 + \Delta\mathbf{B}_0 a_{ym} + \mathbf{H}\mathbf{w} + \mathbf{L}_0\mathbf{q} \tag{30}$$

Note that the system's stability is only decided by the system matrix for $\mathbf{e}$, then the term $\mathbf{L}_0\mathbf{q}$ does not affect the stability and it can be treated as a disturbance. As $\mathbf{H}$ is considered to be the identity matrix, Eq. 30 can be written as:

$$\dot{\mathbf{e}} = (\mathbf{A}_0 - \mathbf{L}_0\mathbf{C}_0)\,\mathbf{e} + \Delta\mathbf{A}_0\mathbf{x}_0 + \Delta\mathbf{B}_0 a_{ym} + \mathbf{H}(\mathbf{w} + \mathbf{L}_0\mathbf{q}) \tag{31}$$

If the system is asymptotically stable, the matrix $\mathbf{L_0}$ exists and is bounded. Then, the term $(\mathbf{w} + \mathbf{L}_0\mathbf{q})$ is also bounded and Eq. 31 can be rewritten as,

$$\dot{\mathbf{e}} = (\mathbf{A}_0 - \mathbf{L}_0\mathbf{C}_0)\,\mathbf{e} + \Delta\mathbf{A}_0\mathbf{x}_0 + \Delta\mathbf{B}_0 a_{ym} + \mathbf{H}\mathbf{w}' \tag{32}$$

where $\mathbf{w}'$ is now the unknown but bounded external disturbance vector.

A new state vector $\xi = [\mathbf{e}, \mathbf{x}_0]^T$ is defined as follows,

$$\dot{\xi} = \mathbf{A}_p\xi + \mathbf{B}_p a_{ym} + \mathbf{H}'\mathbf{w}'' \tag{33}$$

where,

$$\begin{aligned}
\mathbf{A}_p &= \begin{bmatrix} (\mathbf{A}_0 - \mathbf{L}_0\mathbf{C}_0) & \Delta\mathbf{A}_0 \\ \mathbf{0}_{2x2} & \mathbf{A}_0 + \Delta\mathbf{A}_0 \end{bmatrix} \\
\mathbf{B}_p &= \begin{bmatrix} \Delta\mathbf{B}_0 \\ \mathbf{B}_0 + \Delta\mathbf{B}_0 \end{bmatrix} \\
\mathbf{H}' &= \mathbf{I}_{4x4} \\
\mathbf{w}'' &= \begin{bmatrix} \mathbf{w}' & \mathbf{w} \end{bmatrix}^T
\end{aligned} \tag{34}$$

Since the roll angle is the signal to be estimated, the performance of proposed observer is evaluated by its estimation error. Hence, the variable $\mathbf{z}$ in the H_∞ filtering is chosen as:

$$\mathbf{z} = \mathbf{G}\xi \tag{35}$$

with $\mathbf{G} = \begin{bmatrix} 1 & 0 & 0 & 0 \end{bmatrix}$.

The system defined by Eq. (33) depends on the sensor lateral acceleration, a_{ym}, and external disturbance, w. In order to reduce the effect of both inputs on the roll angle estimated, the H_∞ performance is chosen as [23][20]:

$$\|\mathbf{z}\|_\infty^2 < \gamma_1^2 \|a_{ym}\|_\infty^2 + \gamma_1^2\gamma_2^2 \|\mathbf{w}''\|_\infty^2 \tag{36}$$

where γ_1 is the performance index and γ_2 is the weighing factor which determines the relative importance of the effect of two external inputs, a_{ym} and $\mathbf{w}''$, to the estimated error of the output, ϕ.

The principle of H_∞ is to determine a continuous-time filter in the form of (26) such that for all uncertainties the system in (33) is asymptotically stable and the output z satisfies a prescribed H_∞ performance. Hence, the system given in (33) is asymptotically stable and H_∞ performance in (36) for a given γ_1 and γ_2 if there exists a matriz $\mathbf{P}$ symmetric and positive-definite, $\mathbf{P} = \mathbf{P}^T$ and $\mathbf{P} > 0$, satisfying:

$$\begin{bmatrix} \mathbf{P}\mathbf{A}_p + \mathbf{A}_p^T\mathbf{P} & \mathbf{P}\mathbf{B}_p & \mathbf{P}\mathbf{H}' & \mathbf{G}^T \\ * & -\gamma_1^2\mathbf{I} & \mathbf{0} & \mathbf{0} \\ * & * & -\gamma_1^2\gamma_2^2\mathbf{I} & \mathbf{0} \\ * & * & * & -\mathbf{I} \end{bmatrix} < 0 \tag{37}$$

The proof of the previous statement can be found in [23].

The problem to solve Eq. (37) is that matrices $\mathbf{A_p}$ and $\mathbf{B_p}$ depend on parameters uncertainties. If we considered that matrix $\mathbf{P}$ is defined as:

$$\mathbf{P} = \begin{bmatrix} \mathbf{P}_1 & 0_{2x2} \\ 0_{2x2} & \mathbf{P}_2 \end{bmatrix} > 0 \tag{38}$$

the inequality of Eq. (37) becomes:

$$\begin{bmatrix} \mathbf{P_1}(\mathbf{A}_0 & \mathbf{L}_0\mathbf{C}_0) + (\mathbf{A}_0 & \mathbf{L}_0\mathbf{C}_0)^T\mathbf{P_1} & \mathbf{0}_{2x2} & \mathbf{P_1}\Delta\mathbf{B}_0 & \mathbf{P_1}\mathbf{I}_{2x2} & \mathbf{G}(1:2) & \mathbf{P_1}\mathbf{E}_A & \mathbf{0}_{2x2} \\ & * & & \mathbf{P_2}\mathbf{A}_0 + \mathbf{A}_0^T\mathbf{P}_2 & \mathbf{P}_2(\mathbf{B}_0 + \Delta\mathbf{B}_0) & \mathbf{P_2}\mathbf{I}_{2x2} & \mathbf{G}(3:4) & \mathbf{P_2}\mathbf{E}_A & \varepsilon_A\mathbf{F}_A^T \\ & * & & * & \gamma_1^2\mathbf{I}_{1x1} & \mathbf{0}_{1x2} & \mathbf{0}_{1x1} & \mathbf{0}_{1x2} & \mathbf{0}_{1x2} \\ & * & & * & * & \gamma_1^2\gamma_2^2\mathbf{I}_{2x2} & \mathbf{0}_{2x1} & \mathbf{0}_{2x2} & \mathbf{0}_{2x2} \\ & * & & * & * & * & \mathbf{I}_{1x1} & \mathbf{0}_{2x1} & \mathbf{0}_{1x2} \\ & * & & * & * & * & * & \varepsilon_A\mathbf{I}_{2x2} & \mathbf{0}_{2x2} \\ & * & & * & * & * & * & * & \varepsilon_A\mathbf{I}_{2x2} \end{bmatrix} < 0 \tag{39}$$

Furthermore, applying that

$$\mathbf{Q} = \mathbf{P_1}\mathbf{L_0} \tag{40}$$

the condition given in Eq. (39) can be rewritten as:

$$\begin{bmatrix} (\mathbf{P_1}\mathbf{A}_0 & \mathbf{Q}\mathbf{C}_0) + (\mathbf{P_1}\mathbf{A}_0 & \mathbf{Q}\mathbf{C}_0)^T & \mathbf{0}_{2x2} & \mathbf{P_1}\Delta\mathbf{B}_0 & \mathbf{P_1}\mathbf{I}_{2x2} & \mathbf{G}(1:2) \\ & * & & \mathbf{P_2}\mathbf{A}_0 + \mathbf{A}_0^T\mathbf{P}_2 & \mathbf{P}_2(\mathbf{B}_0 + \Delta\mathbf{B}_0) & \mathbf{P_2}\mathbf{I}_{2x2} & \mathbf{G}(3:4) \\ & * & & * & \gamma_1^2\mathbf{I}_{1x1} & \mathbf{0}_{1x2} & \mathbf{0}_{1x1} \\ & * & & * & * & \gamma_1^2\gamma_2^2\mathbf{I}_{2x2} & \mathbf{0}_{2x1} \\ & * & & * & * & * & \mathbf{I}_{1x1} \end{bmatrix} + \\ \begin{bmatrix} \mathbf{P_1}\mathbf{E}_A \\ \mathbf{P_2}\mathbf{E}_A \\ \mathbf{0}_{2x1} \\ \mathbf{0}_{2x2} \\ \mathbf{0}_{2x1} \end{bmatrix} \mathbf{M} \begin{bmatrix} \mathbf{0}_{2x2} & \mathbf{F}_A & \mathbf{0}_{1x2} & \mathbf{0}_{2x2} & \mathbf{0}_{1x2} \end{bmatrix} + \begin{bmatrix} \mathbf{0}_{2x2} \\ (\mathbf{F}_A)^T \\ \mathbf{0}_{2x1} \\ \mathbf{0}_{2x2} \\ \mathbf{0}_{2x1} \end{bmatrix} \mathbf{M} \begin{bmatrix} (\mathbf{P_1}\mathbf{E}_A)^T & (\mathbf{P_2}\mathbf{E}_A)^T & \mathbf{0}_{1x2} & \mathbf{0}_{2x2} & \mathbf{0}_{1x2} \end{bmatrix} < 0 \tag{41}$$

In [16] and [17], it is indicated that if there are real matrices $\mathbf{\Omega} = \mathbf{\Omega}^T$, $\mathbf{L}$ and $\mathbf{H}$ with compatible dimensions and $N(t)$ satisfies that $|N(t)| \leq 1$, then the following condition:

$$\mathbf{\Omega} + \mathbf{L}N(t)\mathbf{H} + \mathbf{H^T}N(t)\mathbf{L^T} < 0 \tag{42}$$

holds if and only if there exists a positive scalar ε such that:

$$\begin{bmatrix} \mathbf{\Omega} & \mathbf{L} & \varepsilon\mathbf{H^T} \\ * & -\varepsilon\mathbf{I} & 0 \\ * & * & -\varepsilon\mathbf{I} \end{bmatrix} < 0 \tag{43}$$

The proof of the previous statement can be found in [24][25].

For inequality (41), we consider that:

$$\mathbf{\Omega_A} = \begin{bmatrix} \mathbf{P_1}\left(\mathbf{A}_0\right. & \left.\mathbf{L}_0\mathbf{C}_0\right) + \left(\mathbf{A}_0\right. & \left.\mathbf{L}_0\mathbf{C}_0\right)^T\mathbf{P_1} & \mathbf{0}_{2x2} & \mathbf{P_1}\Delta\mathbf{B}_0 & \mathbf{P_1}\mathbf{I}_{2x2} & \mathbf{G}(1:2) \\ & * & & \mathbf{P}_2\mathbf{A}_0 + \mathbf{A}_0^T\mathbf{P}_2 & \mathbf{P}_2\left(\mathbf{B}_0 + \Delta\mathbf{B}_0\right) & \mathbf{P}_2\mathbf{I}_{2x2} & \mathbf{G}(3:4) \\ & * & & * & \gamma_1^2\mathbf{I}_{1x1} & \mathbf{0}_{1x2} & \mathbf{0}_{1x1} \\ & * & & * & * & \gamma_1^2\gamma_2^2\mathbf{I}_{2x2} & \mathbf{0}_{2x1} \\ & * & & * & * & * & \mathbf{I}_{1x1} \end{bmatrix} \tag{44}$$

$$\mathbf{L_A} = \begin{bmatrix} \mathbf{P_1}\mathbf{E}_A \\ \mathbf{P}_2\mathbf{E}_A \\ \mathbf{0}_{2x1} \\ \mathbf{0}_{2x2} \\ \mathbf{0}_{2x1} \end{bmatrix} \tag{45}$$

$$\mathbf{H_A} = \begin{bmatrix} \mathbf{0}_{2x2} & \mathbf{F}_A & \mathbf{0}_{1x2} & \mathbf{0}_{2x2} & \mathbf{0}_{1x2} \end{bmatrix} \tag{46}$$

then, inequality (41) is transformed to inequality:

$$\begin{bmatrix} \mathbf{\Omega}_A & \mathbf{L}_A & \varepsilon_A\mathbf{H}_A^T \\ * & -\varepsilon_A\mathbf{I}_{2x2} & \mathbf{0}_{2x2} \\ * & * & -\varepsilon_A\mathbf{I}_{2x2} \end{bmatrix} < 0 \tag{47}$$

Since, the previous inequality still contains uncertainties due to the term $\mathbf{\Delta B_0}$, the same procedure is carried out, then, inequality (47) is transformed

as inequality:

$$\begin{bmatrix} \mathbf{\Omega}_B & \mathbf{L}_B & \varepsilon_B \mathbf{H}_B^T \\ * & -\varepsilon_B \mathbf{I}_{2x2} & 0 \\ * & * & -\varepsilon_B \mathbf{I}_{2x2} \end{bmatrix} < 0 \tag{48}$$

where

$$\mathbf{\Omega}_B = \begin{bmatrix} \mathbf{\Omega}_A & \mathbf{L}_A & \varepsilon_A \mathbf{H}_A^T \\ * & -\varepsilon_A \mathbf{I}_{2x2} & 0 \\ * & * & -\varepsilon_A \mathbf{I}_{2x2} \end{bmatrix} \tag{49}$$

$$\mathbf{L}_B = \begin{bmatrix} \mathbf{P_1 E}_B \\ \mathbf{P}_2 \mathbf{E}_B \\ \mathbf{0}_{1x1} \\ \mathbf{0}_{2x1} \\ \mathbf{0}_{2x1} \\ \mathbf{0}_{2x1} \\ \mathbf{0}_{2x1} \end{bmatrix} \tag{50}$$

$$\mathbf{H}_B = \begin{bmatrix} \mathbf{0}_{1x2} & \mathbf{0}_{1x2} & \mathbf{F}_B & \mathbf{0}_{1x2} & \mathbf{0}_{1x1} & \mathbf{0}_{1x2} & \mathbf{0}_{1x2} \end{bmatrix} \tag{51}$$

Additionally, all the eigenvalues of the closed loop system defined in Eq. (26) should be constrained into a disk (k, q) with radius k and center located at $(-q, 0)$ in the complex plane in order to have a good transient response with relatively less control energy [16] [22]. This condition is satisfied if there exists a positive-definite and symmetric matrix $\mathbf{P}_1$ such that the following inequality is required to be held:

$$\begin{bmatrix} -q\mathbf{P_1} & (\mathbf{P}_1 \mathbf{A}_0 - \mathbf{Q}\mathbf{C}_0) + k\mathbf{P}_1 \\ & -q\mathbf{P}_1 \end{bmatrix} < 0 \tag{52}$$

For a given value of the weighing factor, γ_2, the minimum H_∞ performance index, γ_1, can be obtained by solving the following minimization problem:

$$min\gamma_1^2 \tag{53}$$

subject to Eq. 38, Eq. 48 and Eq. 52.

4. Results and Discussion

A Mercedes Sprinter is used for this research, as depicted in Figure 4. For the experimental results, different sensors were installed in the vehicle as a MSW 250 Nm steering angle sensor from Kistler, a Vbox 3i dual antenna from Racelogic which utilizes two GPS/GLONASS antennas and an Inertial Measurement Unit (IMU). The IMU was installed close to the vehicle COG. The two antennas were installed on the roof and at 90 deg to the vehicle true heading, allowing the system to measure the roll angle. This roll angle value has been considered as Ground Truth and it has been used to validate the proposed estimator.

Table 1 shows the nominal parameters for the experimental vehicle and their maximum uncertainties taken into account. One of main complexity of the problem is to find an observer gain which ensures system convergence for all defined uncertainties and the system satisfies the performance requirements. The solution of LMI problem given by (53) guaranties this condition. The weight factor, γ_2, affects strongly to the modelling error and how the external inputs influence in the estimation errors. Additionally, γ_1 represents the estimation performance. An analysis is carried out to analyze the influence the weight factor, γ_2, and the localization of eigenvalues on results.

Figure 4: Test vehicle equipped with different sensors

If all the eigenvalues of the closed loop system are constrained into a disk $(5, 5)$, the results obtained for index performance and gain observer are given in Table 2 for different values of weight factor, γ_2. We observe that since increasing weight factor, γ_2, decreasing the index performance, γ_1. However, the value of observer gain obtained in each case is very similar. The performance of the proposed roll angle observer has been proved for a real vehicle travelling on a dry pavement with a speed profile which is showed in Figure 5 under a J-turn and slalom manoeuvres as is indicated in Figure 6.

Table 1: Vehicle parameters and their uncertainties

Symbol	Value	Unit
C_R	53071	Nms/rad
m_s	1700	kg
h_{cr}	0.25	m
I_{xx}	1700	kgm^2
K_R	55314	Nms/rad
ΔC_R	20000	Nms/rad
Δm_s	800	kg
Δh_{cr}	0.1	m
ΔK_R	20000	Nm/rad

As the pseudo-roll angle and the roll rate are available, then (see Eq. (26)),

$$\mathbf{y}_{meas} = \begin{bmatrix} \phi_{NN} & \dot{\phi} \end{bmatrix}^T \tag{54}$$

$$\mathbf{C_0} = \begin{bmatrix} 1 & 0 \\ 0 & 1 \end{bmatrix} \tag{55}$$

Figure 7 shows the comparative results for the manoeuvre given in Figure 5 and Figure 6 for the gain observers given in Table 2. For comparison, the vehicle roll angle obtained using dual GPS antenna is taken as Ground Truth. Additionally, the vehicle roll angle obtained directly from NN is also given.

In addition to the graphical evidence, a quantitative analysis that takes into consideration the error for the roll angle estimated has been accomplished. The following equation has been used to represent the norm error

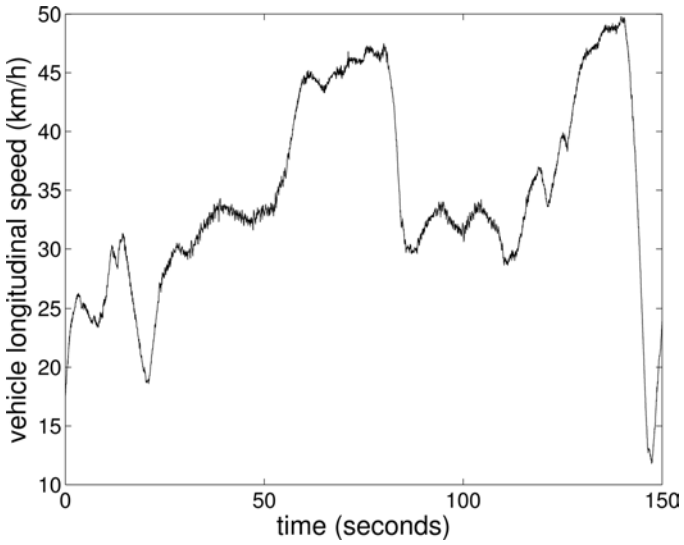

Figure 5: Vehicle speed profile

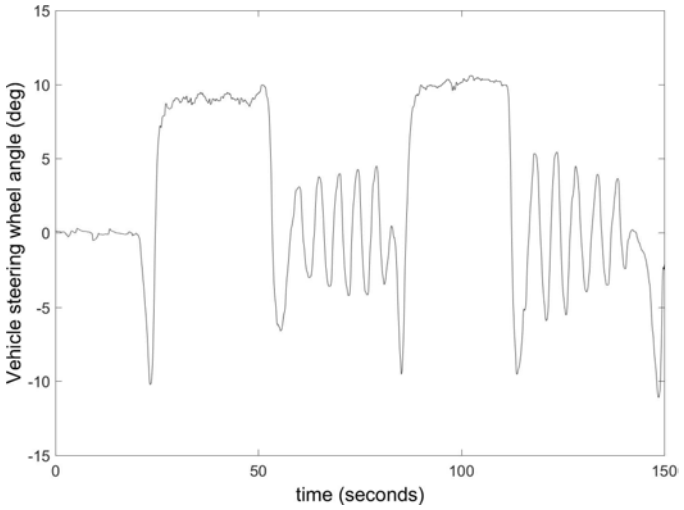

Figure 6: Vehicle steering wheel angle measures with the sensor MSW 250 Nm

as a function of time [26]:

$$E_t = \frac{\varepsilon_t}{\sigma_t} \tag{56}$$

Table 2: H_∞ performance index, γ_1, and observer gain for different values of the weighing factor, γ_2, and considering that the eigenvalues are constrained into a disk $(5, 5)$

CASE	Weight factor γ_2	Index performance γ_1	Observer Gain L_0	Norm error E_t	Maximum error E_{max}, (rad, deg)
1	0.01	10.0039	[9.9998 1.0000 -35.6861 -62.2274]	1.3511	(0.0661, 3.78^o)
2	0.1	1.008	[9.9995 1.0000 -34.4247 -62.2946]	1.3511	(0.0661, 3.78^o)
3	1	0.1	[9.9994 1.0000 -16.8740 -62.9850]	1.3511	(0.0661, 3.78^o)
4	10	0.01	[9.9996 1.0000 -30.4504 -62.3335]	1.3511	(0.0661, 3.78^o)
5	100	0.001	[9.9987 1.0000 -41.1612 -62.0422]	1.3511	(0.0661, 3.78^o)

where,

$$\begin{aligned} \varepsilon_t^2 &= \int_0^T \left(\phi_{\exp} - \phi_{est}\right)^2 dt \\ \sigma_t^2 &= \int_0^T \left(\phi_{\exp} - \mu_{\exp}\right)^2 dt \end{aligned} \tag{57}$$

ϕ_{exp} represents the real vehicle roll angle obtained from the GPS dual antenna (Ground Truth), ϕ_{est} represents the vehicle roll angle obtained from estimator and μ_{exp} is the mean value of the vehicle roll angle obtained from the dual antenna during the period T. The norm and maximum errors are provided in Table 2. The values of norm and maximum errors are the same. Hence, we can conclude that neither the observer gain nor the H_∞-based estimated roll angle are not much affected by the weight factor selected. For this reason, a value γ_2=1 is selected.

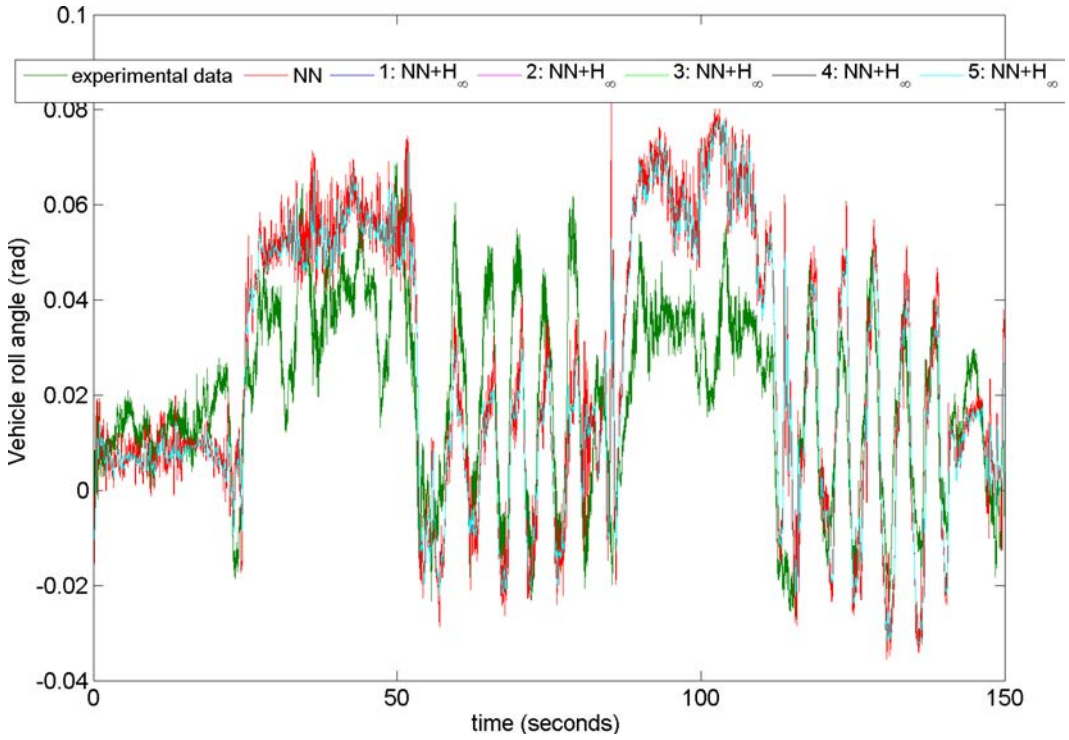

Figure 7: Experimental results for J-turn and Slalom manoeuvres (green points: experimental vehicle roll angle using GPS dual-antenna Ground Truth, red points: vehicle roll angle from NN, rest of colours: vehicle roll angle for cases of Table 2)

In Table 3, results for a given weight factor γ_2=1 and for different constrained disks are shown. In this case, both norm and maximum errors are affected by the selected constrained disk. The higher the circle radius and its center are, the higher errors are obtained.

On the other hand, if we consider the roll angle estimated directly from NN, the obtained norm and maximum errors are 1.9531 and 0.096 rad, respectively (see Table 3). Moreover, we can observe in Figure 8, that a reduction of noise is achieved using a combination of NN and H_∞-based observer (black color) compared with using only NN-based observer (red color).

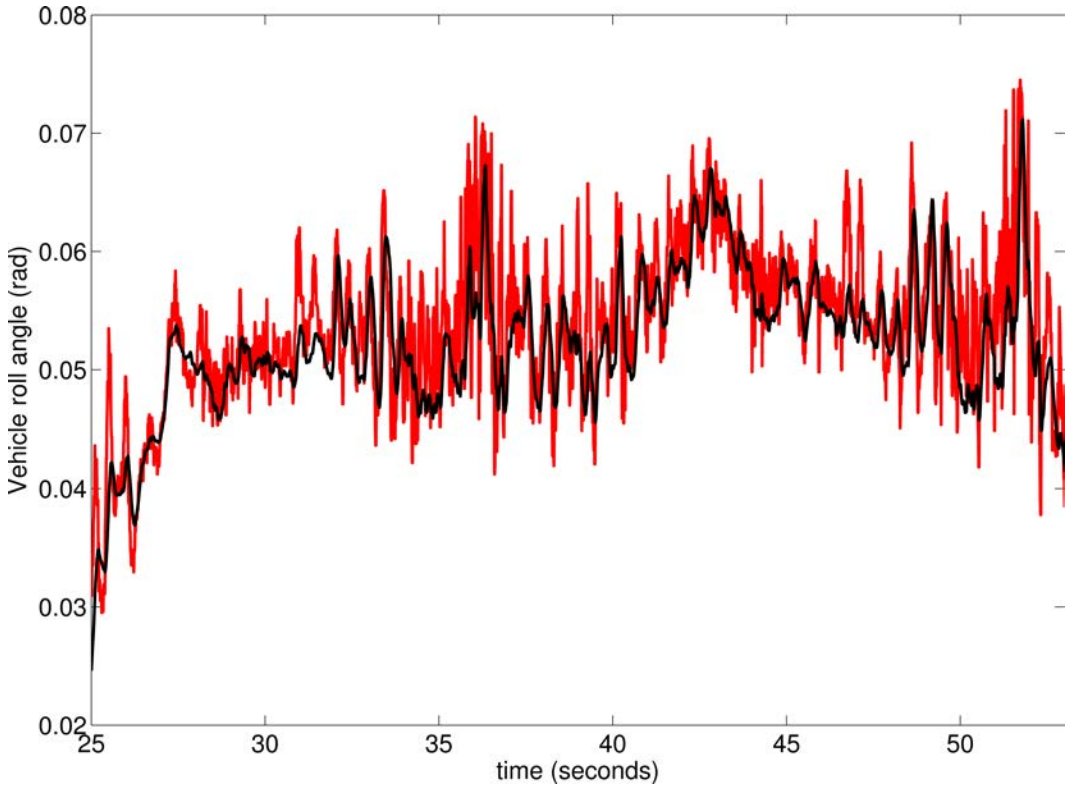

Figure 8: Detail of Figure 7 (red points: vehicle roll angle from NN, black points: vehicle roll angle from NN+H_∞)

Additionally, in order to demonstrate the improvement provided by the proposed algorithm, an estimator based on H_∞ performance, which estimates the vehicle roll angle without considering that the pseudo-roll angle is available, was used for comparison purpose. Hence,

$$\mathbf{y}_{meas} = \left[\dot{\phi}\right]^T \tag{58}$$

$$\mathbf{C_0} = \begin{bmatrix} 0 & 1 \end{bmatrix} \tag{59}$$

For a given value of γ_2=1 and considering that all the eigenvalues of

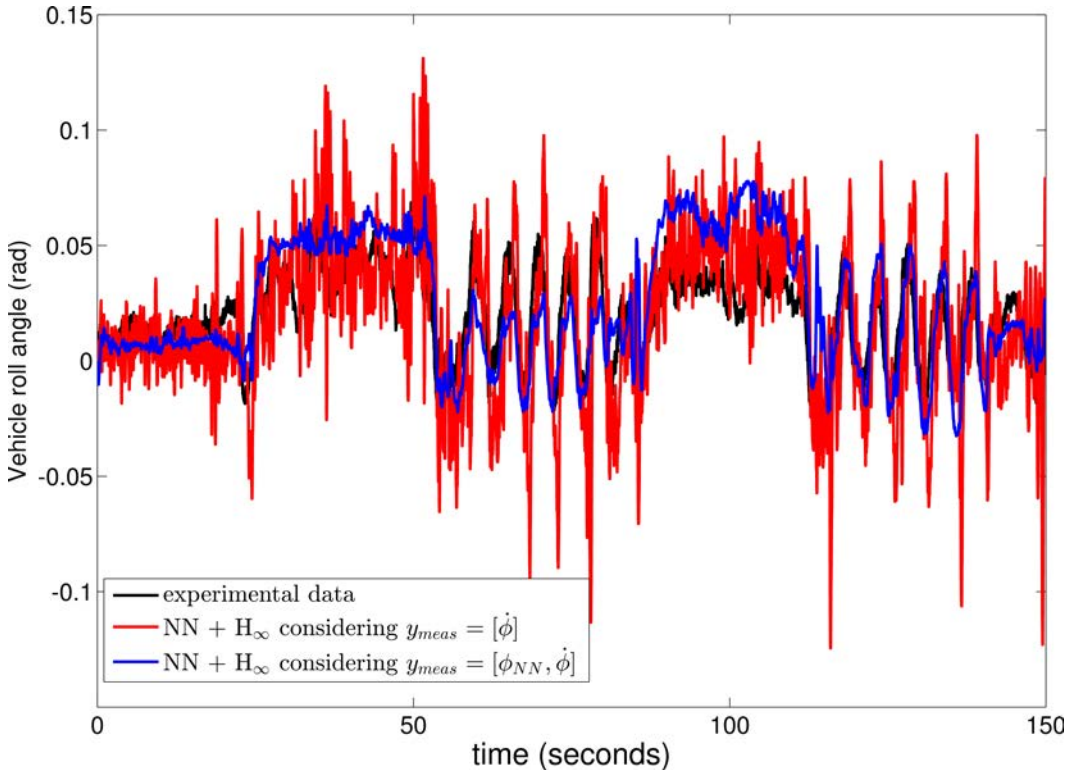

Figure 9: Vehicle roll angle (black points: experimental vehicle roll angle using GPS dual-antenna (Ground Truth), red points: vehicle roll angle using a NN+H_∞-based observer with $\mathbf{y}_{meas} = [\dot{\phi}]$), blue points: vehicle roll angle using a NN+H_∞-based observer with $\mathbf{y}_{meas} = [\phi_{NN}, \dot{\phi}]^T$

the closed loop system are constrained into a disk (5, 5), the calculated performance index is γ_1=1.2528 and the observer gain is

$$\mathbf{L}_0 = \begin{bmatrix} -64.6233 \\ 28.7955 \end{bmatrix} \tag{60}$$

Figure 9 shows the comparative results of H_∞-based observer considering the case when the pseudo-roll angle is available (blue points) and the case when the pseudo-roll angle is not available (red points). Additionally, the

Table 3: Norm error and maximum errors from NN-observer. Observer gain, norm error and maximum error for different constrained disks (k,q) and γ_2=1

CASE	Constrained disk (k,q)	Index performance, γ_1	Observer gain, L_0	Norm error, E_t	Maximum Error, E_{max} (rad, deg)
NN	-	-	-	1.9531	(0.0960, 5.5^o)
NN+H_∞	(5, 5)	0.1	[9.9994 1.0000 -16.8740 -62.9850]	**1.3511**	(**0.0661, 3.78**^{o})
NN+H_∞	(10, 10)	0.05	[19.9979 1.0000 23.6189 -53.8572]	1.5766	(0.0772, 4.42^o)
NN+H_∞	(20, 20)	0.025	[39.9955 1.0000 77.7816 -36.3311]	1.7695	(0.0866, 4.96^o)
NN+H_∞	(50, 50)	0.01	[99.9827 1.0001 291.4116 15.2996]	1.9057	(0.0933, 5.35^o)

vehicle roll angle obtained from GPS dual-antenna, considered as our Ground Truth, is also drawn (black points). The norm and maximum errors for these cases are shown in Table 4. We observe that if only the roll rate is taking into account as measurement, the estimated roll angle is very noisy. Hence, it is necessary the measurement of pseudo-roll angle in order to reduce the noise.

5. Conclusion

A robust H_∞-based observer is proposed to deal with the estimation of vehicle roll angle in presence of parameter uncertainties. This observer uses as measurement the pseudo-roll angle obtained from NN. An important advantage of the proposed observer is that the estimation of pseudo-roll angle

Table 4: Norm and maximum errors considering different available measurements (γ_2=1 and considering that all the eigenvalues of the closed loop system are constrained into a disk (5, 5))

CASE	Norm error, E_t	Maximum error, E_{max} (rad, deg)
$\mathbf{y}_{meas} = [\phi_{NN}, \dot{\phi}]^T$	**1.3511**	(**0.0661, 3.78**^{o})
$\mathbf{y}_{meas} = [\dot{\phi}]$	1.4631	(0.15, 8.59^o)

uses signals of sensors that they are installed onboard in current vehicles. The effectiveness of the proposed observer is shown via a series of comparisons. The proposed NN+H_∞-based observer reduce the noise and errors of the pseudo-roll angle obtained directly from NN. Besides, if only the measurement of roll rate is considered in the estimation of vehicle roll angle, the errors are greater than the errors obtained considering both the measurement of pseudo-roll angle and the measurement of roll rate. Experimental results show the effectiveness of the robust vehicle roll angle observer proposed.

Acknowledgment

This work is supported by the Spanish Government through the Project TRA2013-48030-C2-1-R, which is gratefully acknowledged.

References

[1] M. J. L. Boada, B. L. Boada, A. Munoz, V. Diaz, Integrated control of front-wheel steering and front braking forces on the basis of fuzzy logic, Proceedings of the IMechE 220 (3) (2006) 253–267. doi:10.1243/09544070JAUTO124.

[2] M. J. L. Boada, B. L. Boada, A. Gauchia, J. A. Calvo, V. Diaz, Active roll control using reinforcement learning for a single unit heavy vehicle, Int. J. of Heavy Vehicle Systems 16 (4) (2009) 412–430.

[3] Q. Lu, P. Gentile, A. Tota, A. Sorniotti, P. Gruber, F. Costamagna, J. D. Smet, Enhancing vehicle cornering limit through sideslip and yaw rate control, Mechanical Systems and Signal Processing 75 (2016) 455–472. doi:http://dx.doi.org/10.1016/j.ymssp.2015.11.028.

[4] G. Reina, M. Paiano, J.-L. Blanco-Claraco, Vehicle parameter estimation using a model-based estimator, Mechanical Systems and Signal Processing 87, Part B (2017) 227–241. doi:http://dx.doi.org/10.1016/j.ymssp.2016.06.038.

[5] B. L. Boada, M. J. L. Boada, V. Diaz, Vehicle sideslip angle measurement based on sensor data fusion using an integrated anfis and an unscented kalman filter algorithm, Mechanical Systems and Signal Processing 7273 (2016) 832–845. doi:http://dx.doi.org/10.1016/j.ymssp.2015.11.003.

[6] R. Rajamani, D. N. Piyabongkarn, New paradigms for the integration of yaw stability and rollover prevention functions in vehicle stability control, IEEE Transactions on Intelligent Transportation Systems 14 (1) (2013) 249–261. doi:10.1109/TITS.2012.2215856.

[7] R. Rajamani, D. Piyabongkarn, V. Tsourapas, J. Y. Lew, Parameter and state estimation in vehicle roll dynamics, IEEE Transactions on

Intelligent Transportation Systems 12 (4) (2011) 1558–1567. doi:10.1109/TITS.2011.2164246.

[8] L. Vargas-Melendez, B. Boada, M. Boada, A. Gauchia, V. Diaz, A sensor fusion method based on an integrated neural network and kalman filter for vehicle roll angle estimation, Sensors 16 (9). doi:doi:10.3390/s16091400.

[9] M. Doumiati, G. Baffet, D. Lechner, A. Victorino, A. Charara, Embedded estimation of the tire/road forces and validation in a laboratory vehicle, in: In Proceedings of 9th International Symposium on Advanced Vehicle Control, 2008, pp. 533–538.

[10] K. Jo, K. Chu, M. Sunwoo, Interacting multiple model filter-based sensor fusion of gps with in-vehicle sensors for real-time vehicle positioning, IEEE Transactions on Intelligent Transportation Systems 13 (1) (2012) 329–343. doi:10.1109/TITS.2011.2171033.

[11] D. M. Bevly, J. Ryu, J. C. Gerdes, Integrating ins sensors with gps measurements for continuous estimation of vehicle sideslip, roll, and tire cornering stiffness, IEEE Transactions on Intelligent Transportation Systems 7 (4) (2006) 483–493. doi:10.1109/TITS.2006.883110.

[12] K. Nam, S. Oh, H. Fujimoto, Y. Hori, Estimation of sideslip and roll angles of electric vehicles using lateral tire force sensors through rls and kalman filter approaches, IEEE Transactions on Industrial Electronics 60 (3) (2013) 988–1000. doi:10.1109/TIE.2012.2188874.

[13] S. Zhang, S. Yu, C. Liu, X. Yuan, S. Liu, A dual-linear kalman filter for real-time orientation determination system using low-cost mems sensors, Sensors 16 (2016) 264.

[14] B. L. Boada, D. Garcia-Pozuelo, M. J. L. Boada, V. Diaz, A constrained dual kalman filter based on pdf truncation for estimation of vehicle parameters and road bank angle: Analysis and experimental validation (2016). doi:10.1109/TITS.2016.2594217.

[15] B. Yu, Y. Shi, H. Huang, l_2 - l_∞ filtering for multirate systems based on lifted models, Circuits, Systems and Signal Processing 27 (5) (2008) 699–711. doi:10.1007/s00034-008-9058-3.
URL http://dx.doi.org/10.1007/s00034-008-9058-3

[16] H. Zhang, X. Zhang, J. Wang, Robust gain-scheduling energy-to-peak control of vehicle lateral dynamics stabilisation, Vehicle System Dynamics 52 (3) (2014) 309–340. doi:10.1080/00423114.2013.879190.

[17] H. Zhang, X. Huang, J. Wang, H. R. Karimi, Robust energy-to-peak sideslip angle estimation with applications to ground vehicles, Mechatronics 30 (2015) 338–347. doi:http://dx.doi.org/10.1016/j.mechatronics.2014.08.003.

[18] H. Zhang, A. S. Mehr, Y. Shi, Improved robust energy-to-peak filtering for uncertain linear systems, Signal Processing 90 (9) (2010) 2667–2675. doi:http://dx.doi.org/10.1016/j.sigpro.2010.03.011.

[19] H. Zhang, J. Wang, Vehicle lateral dynamics control through afs/dyc

and robust gain-scheduling approach, IEEE Transactions on Vehicular Technology 65 (1) (2016) 489–494. doi:10.1109/TVT.2015.2391184.

[20] G. Zhang, H. Zhang, X. Huang, J. Wang, H. Yu, R. Graaf, Active fault-tolerant control for electric vehicles with independently driven rear in-wheel motors against certain actuator faults, IEEE Transactions on Control Systems Technology 24 (5) (2016) 1557–1572. doi:10.1109/TCST.2015.2501354.

[21] A. Ferjani, H. Ghorbel, M. Chaabane, A. Rabhi, A. Elhajjaji, Energy-to-peak performance of motorcycle lateral dynamic study, in: 2016 5th International Conference on Systems and Control (ICSC), 2016, pp. 49–54. doi:10.1109/ICoSC.2016.7507048.

[22] G. Zhang, Z. Yu, J. Wang, Correction of contaminated yaw rate signal and estimation of sensor bias for an electric vehicle under normal driving conditions, Mechanical Systems and Signal Processing 87, Part B (2017) 64–80. doi:http://dx.doi.org/10.1016/j.ymssp.2016.05.034.

[23] X. Huang, H. Zhang, G. Zhang, J. Wang, Robust weighted gain-scheduling vehicle lateral motion control with considerations of steering system backlash-type hysteresis, IEEE Transactions on Control Systems Technology 22 (5) (2014) 1740–1753. doi:10.1109/TCST.2014.2317772.

[24] L. Xie, Y. C. Soh, Robust control of linear systems with generalized positive real uncertainty, Automatica 33 (5) (1997) 963–967. doi:http://dx.doi.org/10.1016/S0005-1098(96)00247-6.

[25] X. Jiang, Q.-L. Han, Delay-dependent robust stability for uncertain linear systems with interval time-varying delay, Automatica 42 (6) (2006) 1059–1065. doi:http://dx.doi.org/10.1016/j.automatica.2006.02.019.

[26] M. J. L. Boada, J. A. Calvo, B. L. Boada, V. D?az, Modeling of a magnetorheological damper by recursive lazy learning, International Journal of Non-Linear Mechanics 46 (3) (2011) 479–485. doi:10.1016/j.ijnonlinmec.2008.11.019.